Effect of Longitudinal Reinforcement Ratio on the Behaviour of Deep Beams Reinforced with GFRP Headed-End Bars

Ahmed Bediwy, Karam Mahmoud, and E. El-Salakawy

1 Introduction

In the last century, numerous research have been conducted to understand the behaviour of steel-reinforced concrete (RC) structures. In general, concrete members can be classified into two categories based on shear behavior: slender and deep. Of particular interest, in this paper, is the shear behaviour of deep members containing no distributed web reinforcement. They are well-known with their relatively higher load capacity compared to slender beams. RC structures are exposed to harsh environment especially in North America, which, over time, can cause severe deterioration due to the corrosion problems. Thus, the use of fibre-reinforced polymers (FRP) bars became more common in the last two decades as they are noncorrosive materials [1].

It is well established that in deep beams, which have a shear span-to-depth ratio (*a/d*) less than 2.5 [2, 7], after the formation of the diagonal crack, a significant amount of load is transferred to the supports by a compression thrust linking the load and forming the arch action. In the meantime, the longitudinal reinforcement works as a tie. Such load transfer mechanism is named arch action or strut-and-tie model (STM) [6]. Generally, the glass FRP (GFRP)-RC beams behaves in a similar manner to their steel-RC counterparts [4, 5]. However, with respect to steel bars, the GFRP bars had different characteristics such as relatively low modules of elasticity, which results in wider and deeper cracks that adversely affect the shear capacity of beams

A. Bediwy (✉) · E. El-Salakawy
University of Manitoba, Winnipeg, Canada
e-mail: gabera@myumanitoba.ca

E. El-Salakawy
e-mail: Ehab.El-Salakawy@umanitoba.ca

K. Mahmoud
Fresh Projects Builders, Winnipeg, MB, Canada

Assuit University, Assuit, Egypt

Table 1 Details of test specimens

Beam ID	d^a (mm)	a^b (mm)	a/d	f_c' (MPa)	ρ
B1.4	523	520	1.0	48	1.4
B1.0	523	520	1.0	48	1.0
B0.6	523	520	1.0	47	0.6

[a] d is the effective depth
[b] a is the clear shear span

internally reinforced with GFRP. This paper aims to investigate the shear behaviour of simply supported deep beams reinforced with GFRP bars that do not contain any web reinforcement.

2 Experimental Program

2.1 Test Specimens

Three large scale concrete deep beams reinforced with GFRP bars were constructed and tested to failure. All specimens had a rectangular cross section of 250×590 mm, a/d of 1.0, and an overall length of 3,500 mm. The longitudinal reinforcement ratio, ρ, varied between 1.4, 1.0 and 0.6%. The test specimens were labelled based on the longitudinal reinforcement ratio. For example, Specimen B1.4 is the beam specimen that has $\rho = 1.4\%$. Table 1 lists the details of the specimens.

2.2 Materials Properties

Table 2 shows the properties of the used GFRP reinforcing bars. The headed ends are made of thermoplastic matrix reinforced with short glass fibre, cast at the end of bars at high temperature. The head is approximately 100 mm in length with a maximum outer diameter of 50 mm at the end as shown in Fig. 1. The concrete compressive

Table 2 Mechanical properties of GFRP bars

Bar No.	Diameter (mm)	Area (mm^2)	Tensile strength (MPa)	Modulus of elasticity (GPa)	Ultimate strain (%)
15 M	15.9 (19.2)^a	198 (291)^a	1,184	62.6	1.89
20 M	19 (22.4)^a	285 (394)^a	1,105	63.7	1.73

[a] Diameter and cross-sectional area including sand coating
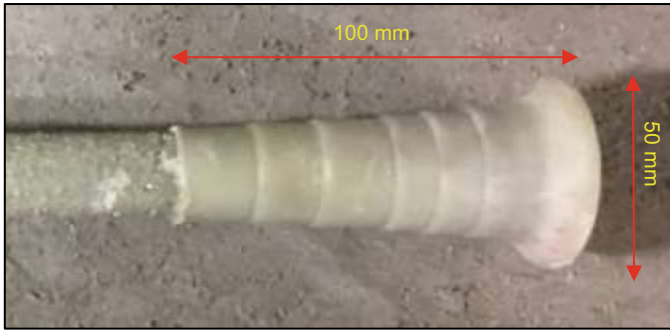
Fig. 1 Configuration of the head

strength was determined on the day of testing according to ASTM C39 [3]. The obtained concrete strengths are listed in Table 1.
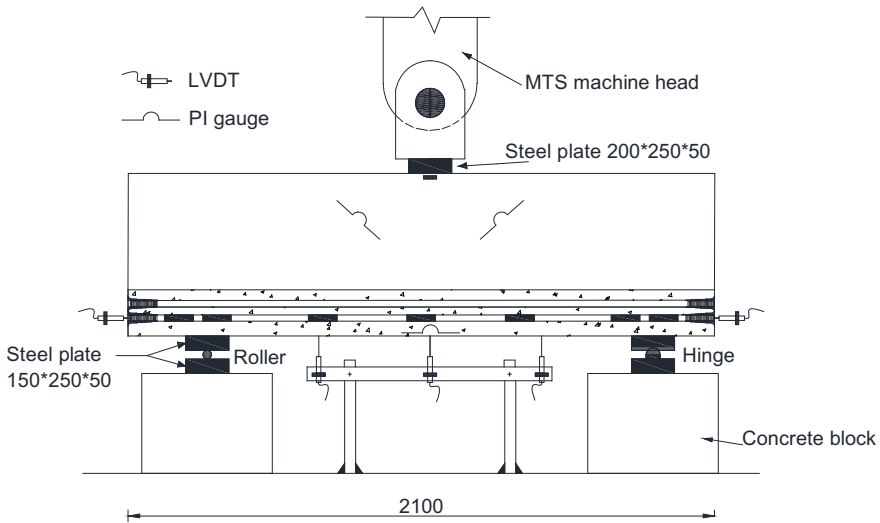
2.3 Test Setup and Instrumentation

The beams were tested under a single monotonic load acting at the mid-span. All specimens were loaded using an MTS loading machine with a capacity of 5,000 kN. Bearing plates were $150 \times 250 \times 50$ mm and $200 \times 250 \times 50$ mm at supports and loading point, respectively.

To capture the strain profile in the reinforcement, seven strain gauges were attached to the reinforcement at critical locations. In addition, five linear variable displacement transducers (LVDTs) were installed, three to measure the deflection, the other two were installed to report any slippage between the FRP bars and the heads. In addition, three PI-gauges were installed to capture the propagation and widening of cracks. All instrumentation was connected to a data acquisition system (DAQ) to record the readings during the test. Figure 2 shows a schematic drawing of the test setup.

3 Test Results and Discussion

3.1 Mode of Failure

At initial stages of loading, 14–16% of ultimate load, flexural cracks were noticed near the mid-span section for all tested beams. As the load increased, such cracks propagated vertically upward to the proximity of mid-height of beam. As loading continued, flexural shear cracks developed in the shear spans. With further loading, cracks became diagonal and parallel to the compression strut connecting the loading

Fig. 2 Test setup and instrumentation (all dimensions are in mm)

point and the support. At high level of loads, the width of the diagonal crack kept increasing until failure, except for B1.4. Failure of diagonal compression strut in the region between the loading and supporting plates occurred in B0.6 and B1.0. The failure for both beams was very brittle and the concrete was broken away or snapped off, as shown in Fig. 3a and b. On the other hand, the beam with high reinforcement ratio, B1.4, experienced premature failure around the loading point as shown in Fig. 3c.

3.2 Load–Deflection

Figure 4 shows the effect of the reinforcement ratio on the load–deflection response of the tested beams. All three specimens exhibited similar overall behavior before the formation of the flexural cracks where the deflection was of very small values. This behaviour was characterized by a nearly bilinear response. After cracking, a reduction in the flexural stiffness of the specimens was observed but with different tendencies, which is attributed to the different reinforcement ratio of each specimen. The figure indicates that as the amount of reinforcement was increased, the post-cracking flexural stiffness increased. Thus, the flexural behaviour of the tested beams, in terms of load–deflection response, seems to be a function of the axial stiffness of the reinforcing bars. Supposedly, an increase in ρ is known to produce a higher shear capacity in deep beams when other design parameters are kept constant. This trend was observed between B1.0 and B0.6. For example, specimen B1.0, which had a reinforcement ratio 67% larger than B0.6 had a stiffer loading response and a higher
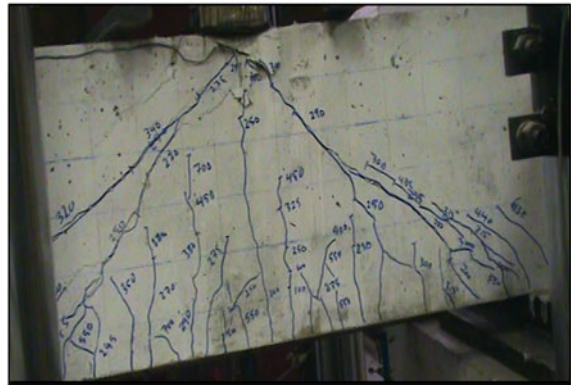
Fig. 3 Failure mechanisms for **a** B0.6, **b** B1.0, and **c** B1.4
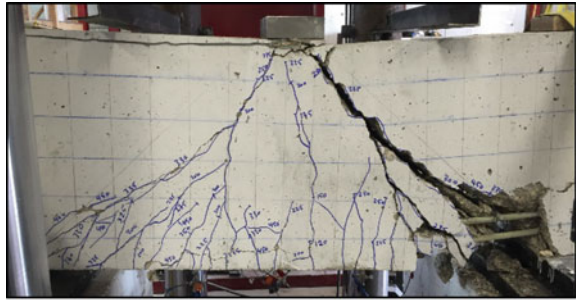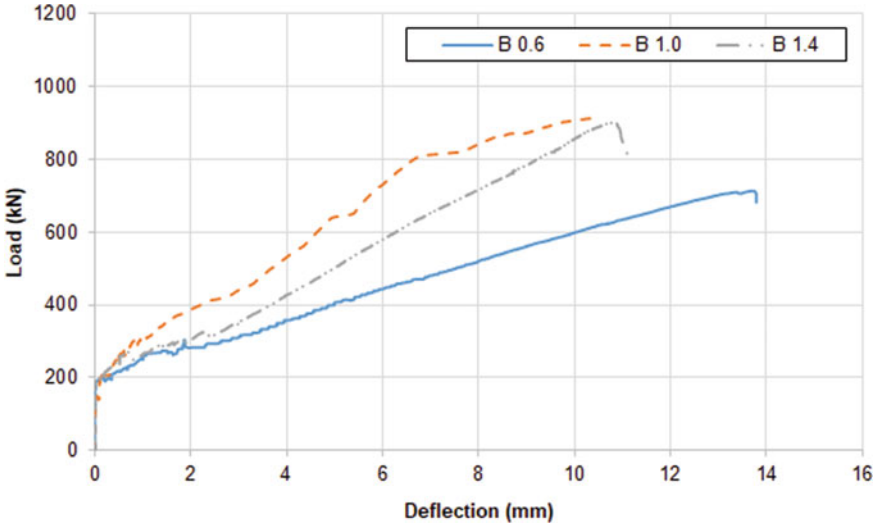

(a)

(b)

(c)

Fig. 4 Load–deflection relationship for tested beams

capacity of about 20%. On the other hand, this trend was not observed, when the load carrying capacity of the two tested beams B1.0 and B1.4 were compared. The failure load for both beams was similar and measured about 900 kN. This was attributed to that a local failure at the loading point due to high compressive stress occurring around the loading point was taken place in B1.4. This failure is recognised as a premature failure, which is not desirable.

4   Conclusions

Based on the presented discussions, the following can be concluded:

1. The mode of failure for B0.6 and B1.0 was brittle reflected by several diagonal cracks in the region between the loading and supporting plates.
2. A premature failure around the loading point was observed for B1.4.
3. During the pre-cracking stage, the load deflection response for all tested beams was similar.
4. The load capacity of the specimens increased as the reinforcement ratio increased, except for B1.4.

References

1. ACI Committee 440 (2015) Guide for the design and construction of structural concrete reinforced with FRP bars. ACI 440.1R-15, American Concrete Institute, Detroit, MI, USA, pp 1–88
2. ASCE-ACI Committee 426 (1973) Shear and diagonal tension. ASCE, J Struct Div 6:1091–1187
3. ASTM (2012) Standard test method for compressive strength of cylindrical concrete specimens. ASTM C39–12, West Conshohocken, PA
4. Manuel R, Slight B, Suter G (1971) Deep beam behavior affected by length and shear span variations. ACI J Proc 68(12):954–958
5. Rogowsky DM, MacGregor JG, Ong SY (1986) Design of reinforced concrete deep beams. ACI J Proc 83(4):614–623
6. Tuchscherer R, Birrcher D, Huizinga M, Bayrak O (2011) Distribution of stirrups across web of deep beams. ACI Struct J 108(6):108–115
7. Wight JK, MacGregor JG (2009) Reinforced concrete: mechanics and design, 6th edn. Pearson Prentice Hall, Upper Saddle River, New Jersey, USA, pp 1–1157